International Journal of Engineering Research and Technology. ISSN 0974-3154, Volume 13, Number 12 (2020), pp. 5066-5077

Performance of a Split Bregman Method for a TVL1-type of Image Restoration Model

Hyo Jin Lim[1] **and Jae Heon Yun**[2,*]

[1,2]*Department of Mathematics, College of Natural Sciences, Chungbuk National University, Cheongju, Korea 28644.*

Abstract

In this paper, we first propose a split Bregman method, using the CGLS (Conjugate gradient least squares method), for solving a TVL1-type of image restoration model with impulse noise, and then we provide a convergence analysis for the split Bregman method. We also provide numerical experiments for several test problems with impulse noise in order to evaluate the performance of the split Bregman method.

Keywords: Total variation, split Bregman method, image restoration, impulse noise, CGLS.

1991 Mathematics Subject Classification: 94A08, 54E05, 49Q20, 35M85.

1. INTRODUCTION

One of the most fundamental problems in image processing and computer vision is image restoration whose main goal is to recover a true image from an observed image. Specifically, we consider the problem of restoring images degraded by blurring and impulse noise. There are two main types of impulse noise which are salt-and-pepper noise and random-valued noise. Assume that an intensity range of an images is $[d_{min}, d_{max}]$. Salt-and-pepper noise corrupts a portion of pixels with only two values of d_{min} or d_{max} while keeping other pixels unaffected. For random-valued noise, a portion of pixels is corrupted in the same manner as salt-and-pepper noise except that the corrupted pixels can take any random value between d_{min} and d_{max}.

Throughout the paper, we assume that the true image U has a square array of size $N \times N$. For convenience of exposition, the true image U is represented by a long vector u of size $m = N^2$ which is obtained by stacking the columns of U. We also assume that an observed (or degraded) image $f \in \mathbb{R}^m$ is represented by

$$f = N_{imp}(Au), \tag{1.1}$$

where $N_{imp}(\cdot)$ denotes the process of image degradation by impulse noise, and $A \in \mathbb{R}^{m\times m}$ is a blurring operator which is generated by a point spread function and a boundary condition imposed outside of the image. In this paper, we only consider the reflexive boundary condition, which means that the scene outside the image boundaries is a mirror image of the scene inside the image boundaries. Our objective of this paper is to restore u from the blurred image f with impulse noise as well as possible.

The classic TVL1 model [9] for recovering a true image u from an observed image f with impulse noise is given by the following variational problem with the l_1-norm fidelity term and total variational regularization term

$$\min_u \Big\{ \|Au - f\|_1 + \mu TV(u) : u \in \mathbb{R}^m \Big\}, \tag{1.2}$$

where $\mu > 0$ is a regularization parameter, A is a blurring matrix and $TV(u)$ denotes the isotropic TV (total variation) norm. Notice that the isotropic TV norm can be represented by $TV(u) = (\varphi \circ B)(u) = \varphi(Bu)$ (see [14] for the detailed descriptions of φ and B).

In the last few decades, the problem of solving the classical TVL1 model (1.2) has been studied by many researchers [3, 5, 9, 10, 12]. It was shown that the TVL1 model (1.2) works successfully in recovering blurred images corrupted by impulse noise. Notice that the TVL1 peoblem (1.2) is very difficult to solve since both the l_1-norm data fidelity term and regularization term are not differentiable.

There have been many mathematical models other than the TVL1 model (1.2) for recovering a true image from an observed image corrupted by blur and impulse noise (see [4, 7, 8, 11, 13, 14]). Recently, Lu et al. [8] proposed the following TVL1 regularization model for image restoration

$$\min_u \Big\{ \|Au - f\|_1 + \frac{\lambda}{2}\|u\|_2^2 + \mu TV(u) \Big\}, \tag{1.3}$$

where λ and μ are positive constants. They showed that the fixed-point method for solving the TVL1 model (1.3) performs remarkably better in the image quality measured by PSNR and preserves more features than FTVd (Fast total variation deconvolution) proposed in [12] at the expense of much increase in computational time.

Motivated by the derivation of the TVL1 model (1.3), Yun and Lim [14] proposed the following image restoration model

$$\min_{u\in\mathbb{R}^m} \Big\{ \|Au - f\|_1 + \frac{\lambda}{2}\|Du\|_2^2 + \mu TV(u) \Big\}, \tag{1.4}$$

where $A \in \mathbb{R}^{m\times m}$ is a blurring matrix, $u \in \mathbb{R}^m$ is a true image, $f \in \mathbb{R}^m$ is a degraded image, λ and μ are positive regularization parameters, $D = -\Delta$ and Δ denote a discrete Laplacian operator. Under the reflexive boundary condition, the negative Laplacian operator D is represented by a singular matrix in $\mathbb{R}^{m\times m}$ (see [14] for the detailed description of D). Throughout the paper, we call the model (1.4) TVL1D2 problem. It was shown in [14] that the fixed-point-like method for solving the TVL1D2 problem performs much better in both PSNR value and CPU time than the fixed-point method for

*Corresponding Author. ORCID: 0000-0001-6841-8137 (Jae Heon Yun)

International Journal of Engineering Research and Technology. ISSN 0974-3154, Volume 13, Number 12 (2020), pp. 5066-5077

solving the TVL1 problem (1.3). Hence, the purpose of this paper is to propose a split Bregman method, using the CGLS (Conjugate gradient least squares method) [1], for solving the TVL1D2 problem.

Notice that the problem (1.3) has a unique solution since its objective function is strictly convex, while the problem (1.4) may not have a unique solution since its objective function is not generally strictly convex.

This paper is organized as follows. In Section 2, we first propose a split Bregman method, using the CGLS, for solving the TVL1D2 problem (1.4), and then we provide a convergence analysis for the split Bregman method. In Section 3, we provide numerical experiments for several test problem in order to evaluate the efficiency and reliability of the split Bregman method for solving the TVL1D2 problem. This can be done by comparing its performance with that of the split Bregman method for solving the TVL1 problem (1.3). Lastly, some conclusion are drawn.

2. SPLIT BREGMAN METHOD FOR THE TVL1D2 PROBLEM

In this section, we first propose a split Bregman method for solving the TVL1D2 problem (1.4), and then we provide a convergence analysis for the split Bregman algorithm. For the basic idea and derivation about the split Bregman method, we refer to [2, 6]. The problem (1.4) can be expressed as

$$\min_u \left\{ \|Au - f\|_1 + \frac{\lambda}{2}\|Du\|_2^2 + \mu\,\varphi(Bu) \right\}. \tag{2.1}$$

The problem (2.1) can be considered as a constrained minimization problem

$$\min_u \left\{ \|h\|_1 + \frac{\lambda}{2}\|Du\|_2^2 + \mu\varphi(d) \right\} \text{ subject to } Bu = d \text{ and } Au - f = h. \tag{2.2}$$

where $d \in \mathbb{R}^{2m}$, $B \in \mathbb{R}^{2m\times m}$ and $h \in \mathbb{R}^{m\times m}$. Rather than considering (2.2), we will consider the following unconstrained optimization problem with a penalty parameters $\gamma,\ \tau > 0$

$$\min_{u,d,h} \left\{ \|h\|_1 + \frac{\lambda}{2}\|Du\|_2^2 + \mu\varphi(d) + \frac{\gamma}{2}\|h - (Au - f) - b\|_2^2 + \frac{\tau}{2}\|d - Bu - c\|_2^2 \right\}. \tag{2.3}$$

Then, the alternating split Bregman method using auxiliary vectors b and c for solving (2.3) can be written as follows:
Given $u^0 = f$ and $h^0 = d^0 = b^0 = c^0 = 0$, the sequence (u^k, h^k, d^k) is generated by the following iteration step

$$\begin{cases} u^{k+1} = \underset{u}{\operatorname{argmin}} \left\{ \frac{\lambda}{2}\|Du\|_2^2 + \frac{\gamma}{2}\|h^k - (Au - f) - b^k\|_2^2 + \frac{\tau}{2}\|d^k - Bu - c^k\|_2^2 \right\}, \\ h^{k+1} = \underset{h}{\operatorname{argmin}} \left\{ \|h\|_1 + \frac{\gamma}{2}\|h - (Au^{k+1} - f) - b^k\|_2^2 \right\}, \\ d^{k+1} = \underset{d}{\operatorname{argmin}} \left\{ \rho\varphi(d) + \frac{\tau}{2}\|d - Bu^{k+1} - c^k\|_2^2 \right\}, \\ b^{k+1} = b^k + \left(Au^{k+1} - f \right) - h^{k+1}, \\ c^{k+1} = c^k + Bu^{k+1} - d^{k+1}. \end{cases} \tag{2.4}$$

We now want to provide a convergence analysis of the split Bregman method defined by (2.4) for the TVL1D2 problem. For this, we note that the first order optimality conditions for the first three equations of (2.4) yield

$$\begin{cases} 0 = \lambda D^T Du^{k+1} - \gamma A^T \left(h^k - (Au^{k+1} - f) - b^k \right) - \tau B^T \left(d^k - Bu^{k+1} - c^k \right), \\ 0 = p^{k+1} + \gamma \left(h^{k+1} - (Au^{k+1} - f) - b^k \right), \\ 0 = \rho q^{k+1} + \tau \left(d^{k+1} - Bu^{k+1} - c^k \right), \\ b^{k+1} = b^k + \left((Au^{k+1} - f) - h^{k+1} \right), \\ c^{k+1} = c^k + \left(Bu^{k+1} - d^{k+1} \right). \end{cases} \tag{2.5}$$

where $p^{k+1} \in \partial\|h^{k+1}\|_1$ and $q^{k+1} \in \partial\varphi(d^{k+1})$. Here the symbol ∂ denotes the subdifferential operator.

Definition 2.1. Let ψ be a convex function and $p \in \partial\psi(v)$. Then the *Bregman distance* is

$$B_\psi^p(u, v) = \psi(u) - \psi(v) - \langle u - v, p\rangle, \tag{2.6}$$

where $\langle\cdot,\cdot\rangle$ stands for the standard inner product.

Lemma 2.2. *Let ψ be a convex function, $d \in \partial\psi(x)$ and $e \in \partial\psi(y)$. Then*

$$\langle x - y, d - e\rangle \geq 0.$$

Proof. Since $B_\psi^d(y,x) = \psi(y) - \psi(x) - \langle y - x, d\rangle$ and $B_\psi^e(x,y) = \psi(x) - \psi(y) - \langle x - y, e\rangle$,

$$\begin{aligned} B_\psi^d(y,x) + B_\psi^e(x,y) &= \psi(y) - \psi(x) - \langle y - x, d\rangle + \psi(x) - \psi(y) - \langle x - y, e\rangle \\ &= \langle x - y, d - e\rangle. \end{aligned}$$

Since all Bregman distances are nonnegative, $\langle x - y, d - e\rangle \geq 0$. □

In the following theorem, we state a convergence property for the split Bregman iteration (2.4), and the detailed proof which can be done using the techniques introduced in [2] is provided in Appendix A.

Theorem 2.3. *Assume that u^* is a solution of the problem* (2.1) *and $\lambda,\ \mu > 0$. Then we have the following convergence property for the split Bregman iteration* (2.4)*:*

$$\begin{aligned} &\lim_{k\to\infty}\Big(\|Au^k - f\|_1 + \frac{\lambda}{2}\|Du^k\|_2^2 + \mu\varphi(Bu^k)\Big) \\ &\qquad = \|Au^* - f\|_1 + \frac{\lambda}{2}\|Du^*\|_2^2 + \mu\varphi(Bu^*) \end{aligned} \tag{2.7}$$

From the iterations step (2.4), we can obtain a split Bregman method, called Algorithm 1, for solving the TVL1D2 problem (1.4).

Algorithm 1 Split Bregman algorithm for the TVL1D2 problem (1.4)

1: Given : observed image f, positive parameters $\gamma,\ \tau,\ \lambda,\ \mu$

2: Initialization : $h^0 = 0$, $b^0 = 0$, $d^0 = 0$, $c^0 = 0$ and $u^0 = f$

3: **for** $k = 0$ to $maxit$ **do**

4: Solve $(\gamma A^TA + \tau B^TB + \lambda D^TD)u^{k+1} = \gamma A^T(h^k - b^k + f) + \tau B^T(d^k - c^k)$ for u^{k+1}

5: $h^{k+1} = \max\{|(Au^{k+1} - f) + b^k| - \frac{1}{\gamma}, 0\}.* sgn((Au^{k+1} - f) + b^k)$

6: **for** $i = 1, 2, \cdots, m$ **do**

7: $$\begin{pmatrix} (d^{k+1})_i \\ (d^{k+1})_{m+i} \end{pmatrix} = \max\left\{\left\|\begin{pmatrix} (Bu^{k+1} + c^k)_i \\ (Bu^{k+1} + c^k)_{m+i} \end{pmatrix}\right\|_2 - \frac{\mu}{\tau}, 0\right\} \cdot \frac{\begin{pmatrix} (Bu^{k+1} + c^k)_i \\ (Bu^{k+1} + c^k)_{m+i} \end{pmatrix}}{\left\|\begin{pmatrix} (Bu^{k+1} + c^k)_i \\ (Bu^{k+1} + c^k)_{m+i} \end{pmatrix}\right\|_2}$$

8: **end for**

9: $b^{k+1} = b^k + (Au^{k+1} - f) - h^{k+1}$

10: $c^{k+1} = c^k + Bu^{k+1} - d^{k+1}$

11: **if** $\frac{\|u^{k+1} - u^k\|_2}{\|u^{k+1}\|_2} < tol$ **then**

12: Stop

13: **end if**

14: **end for**

Notice that the linear system in line 4 of Algorithm 1, which can be viewed as a least squares problem, is approximately solved using the CGLS with a tolerance value (e.g., see [14]). The symbol $.*$ in line 5 of Algorithm 1 denotes elementwise multiplication.

If the matrix D in line 4 of Algorithm 1 is replaced with an identity matrix I, then we obtain Algorithm 1 which is the split Bregman method for solving the TVL1 problem (1.3). From Theorem 2.3, we can easily obtain the following corollary which guarantees the convergence of Algorithm 1.

Corollary 2.4. *Assume that u^* is a unique solution of the problem* (1.3) *and $\lambda,\ \mu > 0$. Then we have the following convergence property for* Algorithm 1*:*

$$\lim_{k\to\infty}\Big(\|Au^k - f\|_1 + \frac{\lambda}{2}\|u^k\|_2^2 + \mu\varphi(Bu^k)\Big) = \|Au^* - f\|_1 + \frac{\lambda}{2}\|u^*\|_2^2 + \mu\varphi(Bu^*).$$

Furthermore, $\lim_{k\to\infty}\|u^k - u^*\|_2 = 0$.

3. NUMERICAL EXPERIMENTS

In this section, we provide numerical experiments for several test problems to evaluate the efficiency and reliability of the split Bregman method (i.e., Algorithm 1). This can be done by comparing its numerical results with those of Algorithm 1. Numerical experiments have been done for five test images such as "Cameraman (Cam)", "Lena", "House", "Boat" and "Pepper". The pixel size of five test images is 256×256. All numerical tests have been performed using Matlab R2016a on a personal computer with Intel(R) Core(TM) i5-3337U CPU and 8.00GB RAM. $maxit$ is set to 500, and *tol* is set to 2×10^{-4}. For the CGLS method which is used to solve a linear system every iteration of Algorithm 1, the tolerance for stopping criterion is set to 5×10^{-2} and the maximum number of iterations is set to 120.

To evaluate the quality of the restored image, we use the PSNR (Peak Singal to Noise Ratio) value between the restored image and original image which is defined by

$$\text{PSNR} = \log_{10}\left(\frac{M \cdot N \cdot max_{i,j}|u_{ij}|^2}{\|U - \tilde{U}\|_F^2}\right),$$

where $\|\cdot\|_F$ refers to the Frobenius norm, U and $\tilde{U}$ are the original and restored image with size $M \times N$, respectively. In addition, u_{ij} stands for the value of original image U at the pixel point (i, j) and $M \cdot N$ is the total number of pixels. It is generally true that the larger PSNR value stands for the better quality of restored image.

For all numerical experiments, we have used the test images with an intensity range of $[0, 1]$. For all test problems, we choose the degraded images which are resulting images blurred by Gaussian kernel of size 15×15 with standard deviation 9 under the reflexive boundary condition, and then corrupted by salt-and-pepper impulse noise with noise levels 20%, 30%, or 60%. In Tables 1 to 3, "Alg." represents the algorithm number to be used, "P_0" represents the PSNR value for the blurred and noisy image f, "Iter" denotes the number of iterations required for each algorithm, parameters "γ, τ, λ and μ" are chosen as the best one by numerical tries, and "Time" denotes the elapsed CPU time in seconds.

Tables 1 to 3 contain numerical results for the split Bregman methods (i.e., Algorithm 1) for degraded images with 20%, 30% or 60% salt-and-pepper impulse noise. In Figures 1 to 5, the first row contains the images restored by Algorithm 1 for blurred images with 60% salt-and-pepper noise, and the second row contains the images restored by Algorithm 1 for blurred images with 30% salt-and-pepper noise.

Algorithm 1 restores the true image better than Algorithm 1 takes less CPU time than Algorithm 1 in most cases (see Tables 1 to 3 and Figures 1 to 5). This means that the split Bregman method for the TVL1D2 problem (1.4) performs better in both PSNR value and CPU time than the split Bregman method for the TVL1 problem (1.3). As can be seen from numerical results in [14], Algorithm 1 restores the true image as well as the fixed-point-like method proposed for the TVL1D2 problem (1.4)

Table 1: Numerical results of the split-Bregman methods for 60% salt-and-pepper noise

Image	P_0	Alg.	γ	τ	μ	λ	tol	PSNR	Iter	Time
Cam	7.11	0	40	0.006	0.014	0.007	1×10^{-5}	24.86	266	714
		1	7	0.002	0.013	0.004	2×10^{-4}	24.94	318	812
Lena	7.12	0	40	0.006	0.016	0.007	1×10^{-5}	26.37	311	799
		1	90	0.02	0.014	0.01	2×10^{-4}	26.54	197	378
House	7.11	0	41	0.005	0.016	0.009	1×10^{-5}	31.10	248	731
		1	40	0.009	0.015	0.01	2×10^{-4}	31.55	167	425
Boat	6.76	0	38	0.02	0.015	0.02	1×10^{-5}	24.70	165	311
		1	50	0.0004	0.012	0.02	2×10^{-4}	25.19	299	1125
Pepper	7.40	0	41	0.006	0.016	0.003	1×10^{-5}	27.78	367	1139
		1	16	0.002	0.015	0.004	2×10^{-4}	28.00	354	1164

Table 2: Numerical results of the split-Bregman methods for 30% salt-and-pepper noise

Image	P_0	Alg.	γ	τ	μ	λ	tol	PSNR	Iter	Time
Cam	9.86	0	108	0.002	0.003	0.0002	1×10^{-5}	30.49	384	1827
		1	394	0.002	0.0027	0.0004	2×10^{-4}	30.49	386	1290
Lena	9.92	0	109	0.002	0.003	0.0002	1×10^{-5}	30.29	362	1911
		1	350	0.007	0.0026	0.001	2×10^{-4}	30.34	268	1156
House	9.91	0	250	0.0002	0.0032	0.005	1×10^{-5}	36.67	353	1576
		1	350	0.0008	0.0027	0.004	2×10^{-4}	37.18	261	1129
Boat	9.55	0	108	0.002	0.003	0.0002	1×10^{-5}	30.50	355	1727
		1	360	0.008	0.0027	0.002	2×10^{-4}	30.76	229	929
Pepper	10.13	0	109	0.002	0.003	0.0003	1×10^{-5}	34.61	342	1644
		1	460	0.002	0.003	0.0008	2×10^{-4}	34.77	368	1640

Table 3: Numerical results of the split-Bregman methods for 20% salt-and-pepper noise

Image	P_0	Alg.	γ	τ	μ	λ	tol	PSNR	Iter	Time
Cam	11.42	0	111	0.001	0.002	0.00006	1×10^{-5}	32.91	355	2389
		1	470	0.1	0.0017	0.0001	2×10^{-4}	33.05	390	1536
Lena	11.52	0	114	0.001	0.002	0.0002	1×10^{-5}	32.28	387	4681
		1	300	0.1	0.0015	0.0001	2×10^{-4}	32.34	308	1226
House	11.54	0	111	0.001	0.002	0.00005	1×10^{-5}	38.24	366	1870
		1	400	0.2	0.0015	0.0025	2×10^{-4}	38.61	172	555
Boat	11.42	0	110	0.001	0.001	0.00002	1×10^{-5}	32.97	373	1772
		1	400	0.1	0.0017	0.0005	2×10^{-4}	33.19	271	1021
Pepper	11.65	0	113	0.001	0.002	0.00005	1×10^{-5}	37.04	386	2461
		1	470	0.1	0.0019	0.0001	2×10^{-4}	37.12	390	1536

International Journal of Engineering Research and Technology. ISSN 0974-3154, Volume 13, Number 12 (2020), pp. 5066-5077

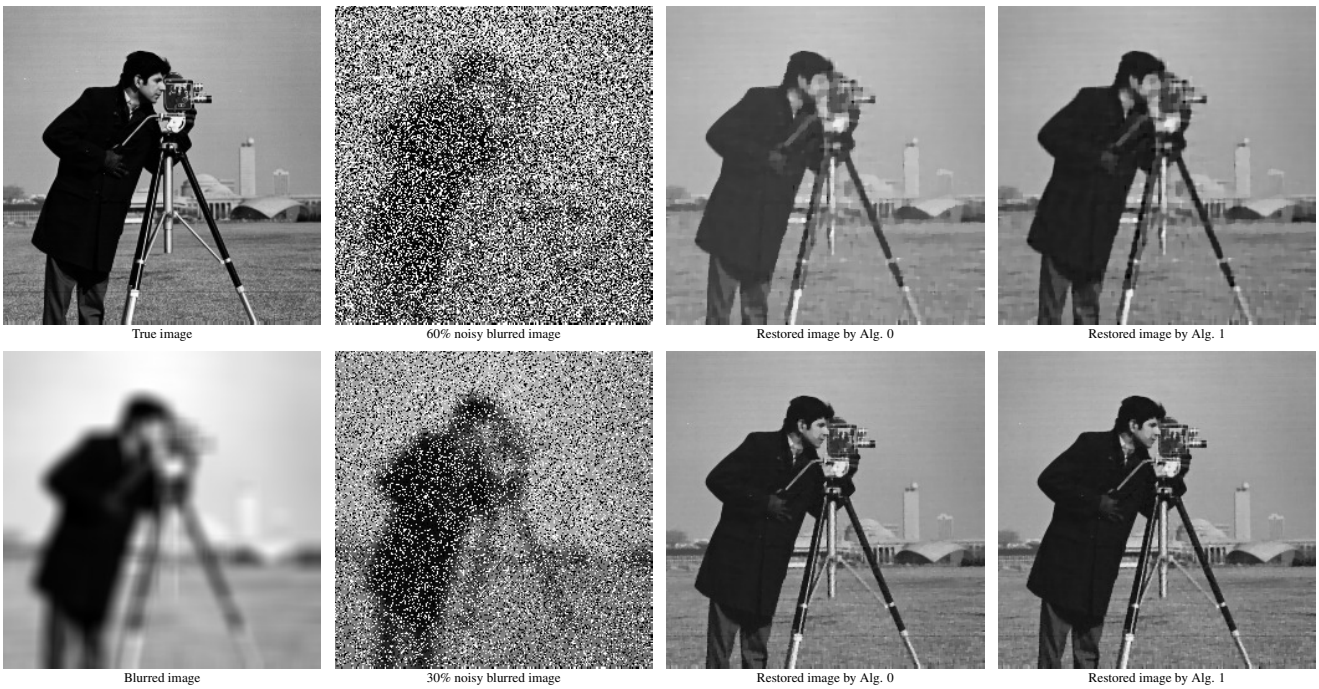

Figure 1: Image restoration by split Bregman methods for blurred Cameraman image with 60% or 30% salt-and-pepper noise.

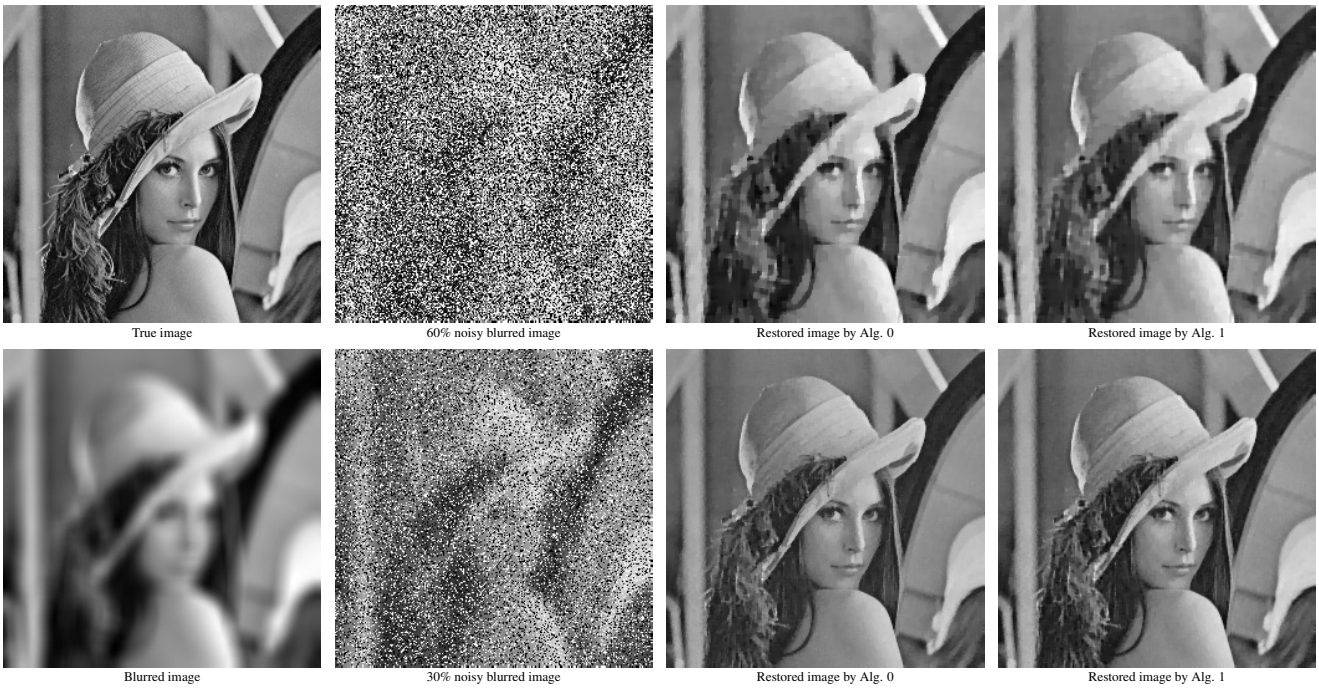

Figure 2: Image restoration by split Bregman methods for blurred Lena image with 60% or 30% salt-and-pepper noise

.

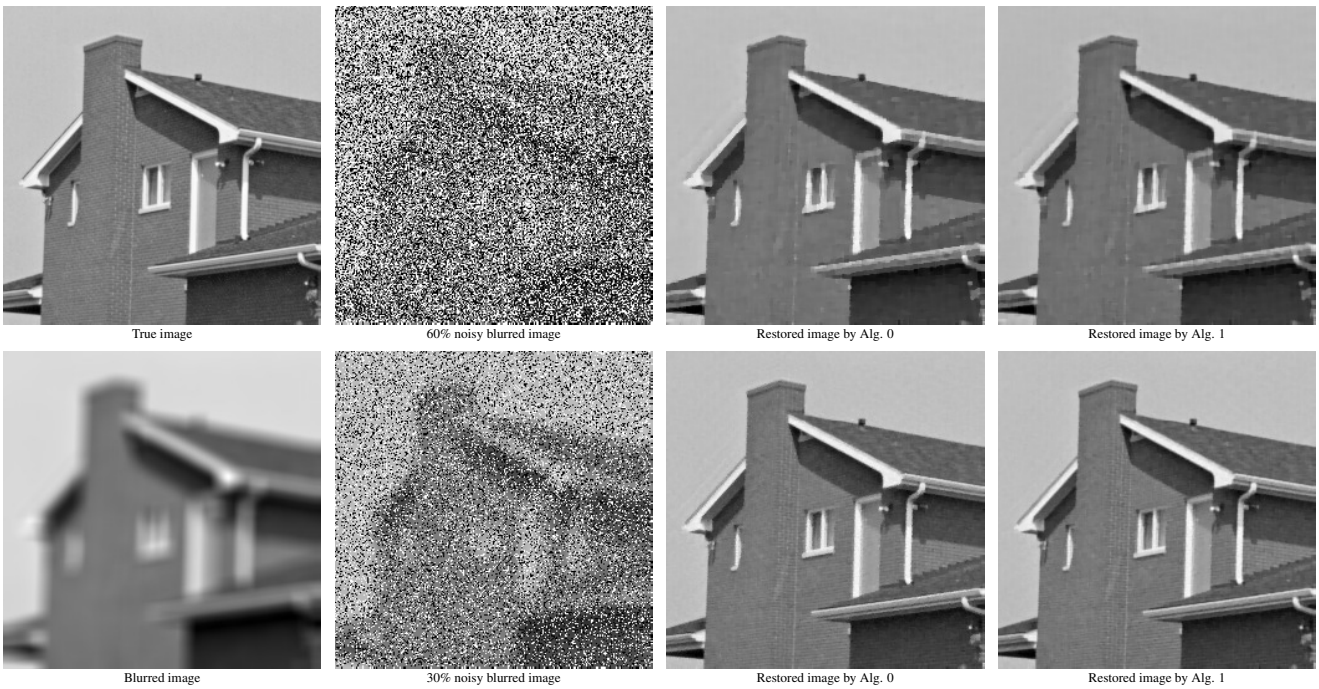

Figure 3: Image restoration by split Bregman methods for blurred House image with 60% or 30% salt-and-pepper noise

.

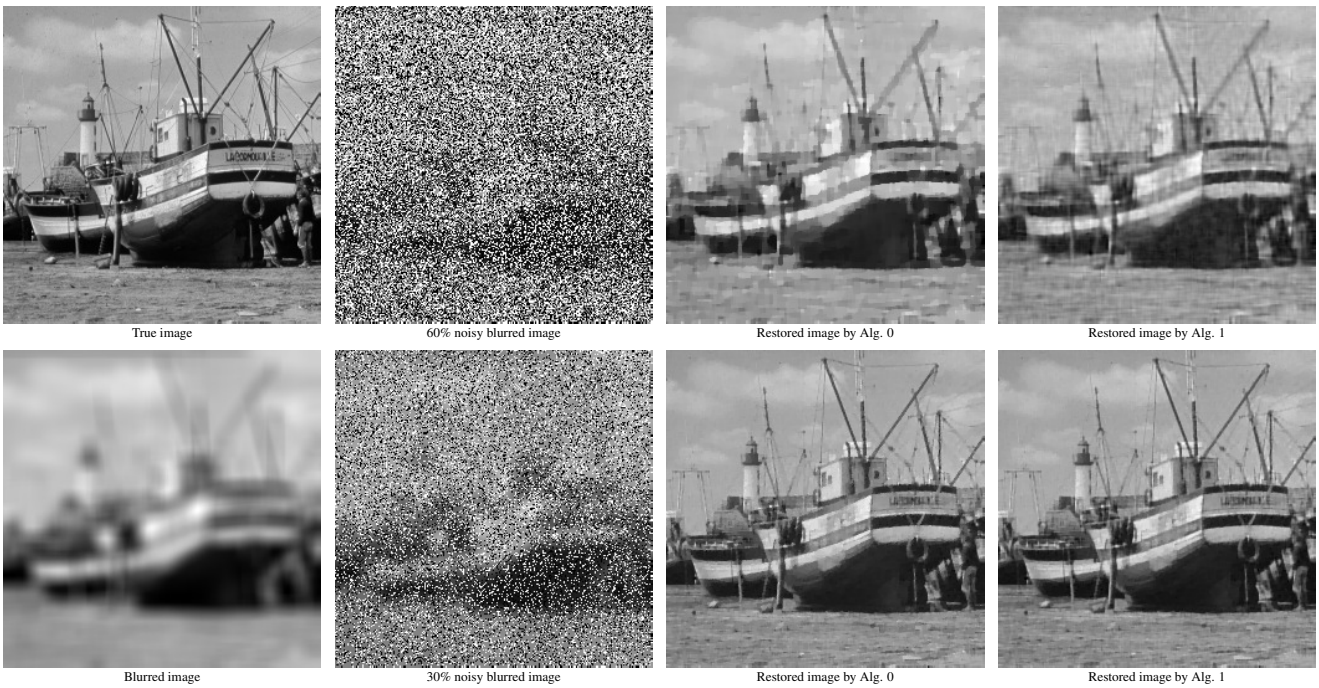

Figure 4: Image restoration by split Bregman methods for blurred Boat image with 60% or 30% salt-and-pepper noise

.

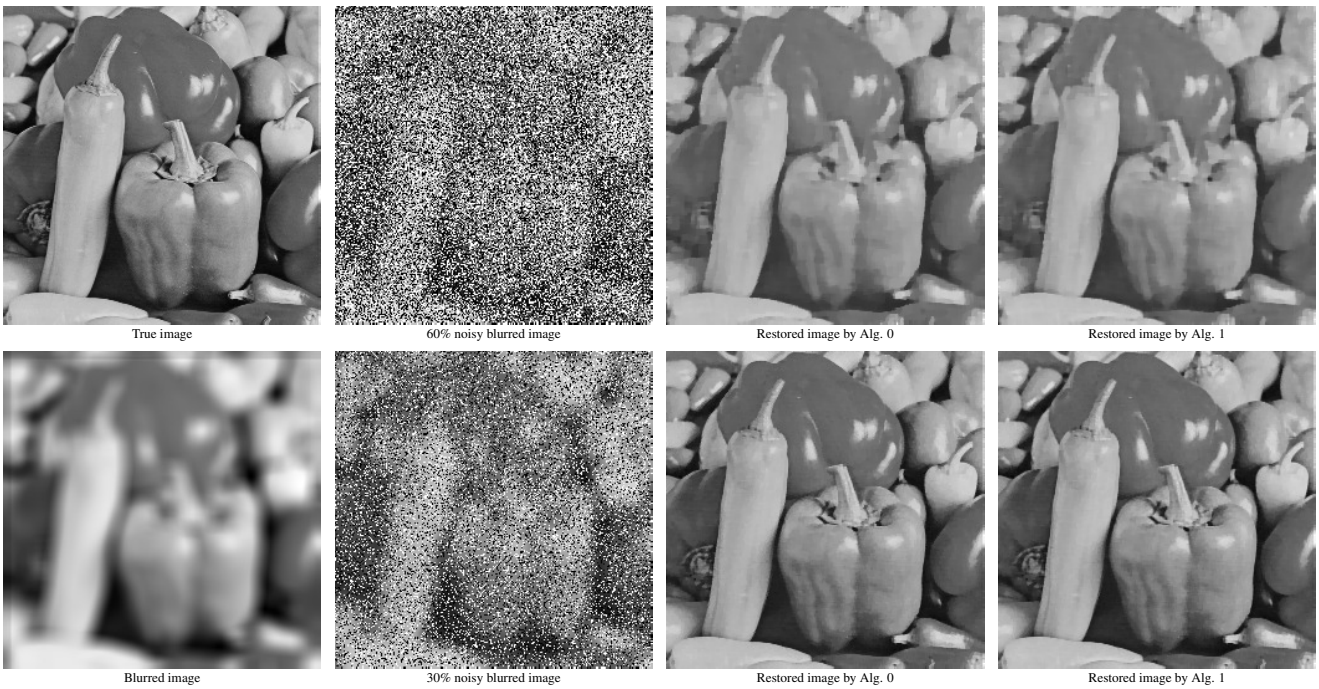

Figure 5: Image restoration by split Bregman methods for blurred Pepper image with 60% or 30% salt-and-pepper noise

.

4. CONCLUSIONS

In this paper, we proposed a split Bregman method, using the CGLS, for solving the TVL1D2 problem (1.4) with impulse noise. Numerical experiments showed that the split Bregman method (i.e., Algorithm 1) for the TVL1D2 problem performs better in both PSNR value and CPU time than the split Bregman method (i.e., Algorithm 0) for the TVL1 problem (1.3). Also Algorithm 1 restores the true image as well as the fixed-point-like method proposed for the TVL1D2 problem (see [14]). Hence, for image restoration problem with impulse noise, the TVL1D2 model is preferred over the existing TVL1 model (1.3), and it is recommended to use Algorithm 1.

The split Bregman method proposed for the TVL1D2 model can be applied to an image inpainting problem or image denoising problem with impulse noise. Future work will study these kinds of problems.

APPENDIX A

Proof of Theorem 2.3. Using the Fermat rule for the minimization problem (2.1), u^* must satisfy

$$0 \in A^T \partial(\|Au^* - f\|_1) + \lambda D^T(Du^*) + \mu B^T \circ \partial\varphi(Bu^*). \tag{4.1}$$

From (4.1), we can obtain the following equality

$$0 = A^T p^* + \lambda D^T(Du^*) + \mu B^T q^*. \tag{4.2}$$

where $p^* \in \partial(\|Au^* - f\|_1)$ and $q^* \in \partial\varphi(Bu^*)$. Let $b^* = \frac{1}{\gamma}p^*$ and $c^* = \frac{\mu}{\tau}q^*$. Since $d^* = Bu^*$ and $h^* = Au^* - f$, from (4.2) we can obtain the following equations

$$\begin{cases} 0 = \lambda D^T Du^* - \gamma A^T\Big(h^* - (Au^* - f) - b^*\Big) - \tau B^T\Big(d^* - Bu^* - c^*\Big), \\ 0 = p^* + \gamma\Big(h^* - (Au^* - f) - b^*\Big), \\ 0 = \mu q^* + \tau\Big(d^* - Bu^* - c^*\Big), \\ b^* = b^* + \Big((Au^* - f) - h^*\Big), \\ c^* = c^* + \Big(Bu^* - d^*\Big). \end{cases} \tag{4.3}$$

(4.3) means that $\{u^*, h^*, d^*, b^*, c^*\}$ is a fixed point set of the split Bregman iteration (2.4).

Let us define the errors $u_e^k = u^k - u^*$, $h_e^k = A(u^k - u^*)$, $d_e^k = d^k - d^*$, $b_e^k = b^k - b^*$ and $c_e^k = c^k - c^*$. All equations of (4.3)

subtracted from those of (2.5) correspondingly show that

$$\begin{cases} 0 = \lambda D^T D u_e^{k+1} - \gamma A\Big(h_e^k - Au_e^k - b_e^k\Big) - \tau B^T\Big(d_e^k - Bu_e^{k+1} - c_e^k\Big), \\ 0 = \Big(p^{k+1} - p^*\Big) + \gamma\Big(h_e^{k+1} - Au_e^{k+1} - b_e^k\Big), \\ 0 = \mu\Big(q^{k+1} - q^*\Big) + \tau\Big(d_e^{k+1} - Bu_e^{k+1} - c_e^k\Big), \\ b_e^{k+1} = b_e^k + \Big(Au_e^{k+1} - h_e^{k+1}\Big), \\ c_e^{k+1} = c_e^k + \Big(Bu_e^{k+1} - d_e^{k+1}\Big). \end{cases} \tag{4.4}$$

Taking the inner products for both sides of the first three equations of (4.4) with respect to u_e^{k+1}, h_e^{k+1} and d_e^{k+1} respectively, we have

$$\begin{cases} 0 = \lambda\|Du_e^{k+1}\|_2^2 + \gamma|Au_e^k\|_2^2 - \tau\|Bu_e^{k+1}\|_2^2 \\ \quad - \gamma\langle h_e^k, Au_e^{k+1}\rangle + \gamma\langle b_e^k, Au_e^{k+1}\rangle - \tau\langle d_e^k, Bu_e^{k+1}\rangle + \tau\langle c_e^k, Bu_e^{k+1}\rangle, \\ 0 = \langle p^{k+1} - p^*, h_e^k\rangle + \gamma\|h_e^{k+1}\|_2^2 - \gamma\langle Au_e^{k+1}, h_e^{k+1}\rangle - \gamma\langle b_e^k, h_e^k\rangle, \\ 0 = \mu\langle q^{k+1} - q^*, d_e^{k+1}\rangle + \tau\|d_e^{k+1}\|_2^2 - \tau\langle Bu_e^{k+1}, d_e^{k+1}\rangle - \tau\langle c_e^k, d_e^k\rangle. \end{cases} \tag{4.5}$$

Squaring both sides of the last two equations of (4.4) yields the following equalities

$$\begin{aligned} \|b_e^{k+1}\|_2^2 &= \|b_e^k\|_2^2 + \|Au_e^{k+1} - h_e^{k+1}\|_2^2 + 2\langle b_e^k, Au_e^{k+1} - h_e^{k+1}\rangle, \\ \|c_e^{k+1}\|_2^2 &= \|c_e^k\|_2^2 + \|Bu_e^{k+1} - d_e^{k+1}\|_2^2 + 2\langle c_e^k, Bu_e^{k+1} - d_e^{k+1}\rangle. \end{aligned} \tag{4.6}$$

Summing all three equations in (4.5) gives us

$$\begin{aligned} 0 = {} & \lambda\|Du_e^{k+1}\|_2^2 + \langle p^{k+1} - p^*, h_e^{k+1}\rangle + \mu\langle q^{k+1} - q^*, d_e^{k+1}\rangle \\ & + \gamma\Big(\|Au_e^{k+1}\|_2^2 + \|h_e^{k+1}\|_2^2 - \langle Au_e^{k+1}, h_e^{k+1} + h_e^k\rangle + \langle b_e^k, Au_e^{k+1} - h_e^{k+1}\rangle\Big) \\ & + \tau\Big(\|Bu_e^{k+1}\|_2^2 + \|d_e^{k+1}\|_2^2 - \langle Bu_e^{k+1}, d_e^{k+1} + d_e^k\rangle + \langle c_e^k, Bu_e^{k+1} - d_e^{k+1}\rangle\Big). \end{aligned} \tag{4.7}$$

Note that two equalities of (4.6) can be reformulated as

$$\begin{aligned} \langle b_e^k, Au_e^{k+1} - h_e^{k+1}\rangle &= \frac{1}{2}\Big(\|b_e^{k+1}\|_2^2 - \|b_e^k\|_2^2\Big) - \frac{1}{2}\|Au_e^{k+1} - h_e^{k+1}\|_2^2, \\ \langle c_e^k, Bu_e^{k+1} - d_e^{k+1}\rangle &= \frac{1}{2}\Big(\|c_e^{k+1}\|_2^2 - \|c_e^k\|_2^2\Big) - \frac{1}{2}\|Bu_e^{k+1} - d_e^{k+1}\|_2^2. \end{aligned} \tag{4.8}$$

Substituting (4.8) into (4.7) yields

$$\begin{aligned} 0 = {} & \lambda\|Du_e^{k+1}\|_2^2 + \langle p^{k+1} - p^*, h_e^{k+1}\rangle + \mu\langle q^{k+1} - q^*, d_e^{k+1}\rangle \\ & + \gamma\Bigg(\|Au_2^{k+1}\|_2^2 + \|h_e^{k+1}\|_2^2 - \langle Au_e^{k+1}, h_e^{k+1} + h_e^k\rangle \\ & \quad + \frac{1}{2}(\|b_e^{k+1}\|_2^2 - \|b_e^k\|_2^2) - \frac{1}{2}\|Au_e^{k+1} - h_e^{k+1}\|_2^2\Bigg) \\ & + \tau\Bigg(\|Bu_e^{k+1}\|_2^2 + \|d_e^{k+1}\|_2^2 - \langle Bu_e^{k+1}, d_e^{k+1} + d_e^k\rangle \\ & \quad + \frac{1}{2}(\|c_e^{k+1}\|_2^2 - \|c_e^k\|_2^2) - \frac{1}{2}\|Bu_e^{k+1} - d_e^{k+1}\|_2^2\Bigg). \end{aligned} \tag{4.9}$$

On the other hand, some computational manipulation gives

$$\begin{aligned} & \gamma\|Au_e^{k+1}\|_2^2 + \gamma\|h_e^{k+1}\|_2^2 - \gamma\langle Au_e^{k+1}, h_e^{k+1} + h_e^k\rangle - \frac{\gamma}{2}\|Au_e^{k+1} - h_e^{k+1}\|_2^2 \\ & = \frac{\gamma}{2}\|Au_e^{k+1}\|_2^2 + \frac{\gamma}{2}\|Au_e^{k+1}\|_2^2 + \frac{\gamma}{2}\|h_e^{k+1}\|_2^2 + \frac{\gamma}{2}\|h_e^{k+1}\|_2^2 \\ & \quad - \gamma\langle Au_e^{k+1}, h_e^{k+1}\rangle - \gamma\langle Au_e^{k+1}, h_e^k\rangle - \frac{\gamma}{2}\|Au_e^{k+1} - h_e^{k+1}\|_2^2 \\ & = \frac{\gamma}{2}\|Au_e^{k+1}\|_2^2 + \frac{\gamma}{2}\|h_e^{k+1}\|_2^2 - \gamma\langle Au_e^{k+1}, h_e^k\rangle + \frac{\gamma}{2}\|h_e^k\|_2^2 - \frac{\gamma}{2}\|h_e^k\|_2^2 \\ & = \frac{\gamma}{2}\|Au_e^{k+1} - h_e^k\|_2^2 + \frac{\gamma}{2}\|h_e^{k+1}\|_2^2 - \frac{\gamma}{2}\|h_e^k\|_2^2 \end{aligned} \tag{4.10}$$

and

$$\begin{aligned}
&\tau\|Bu_e^{k+1}\|_2^2+\tau\|d_e^{k+1}\|_2^2-\tau\langle Bu_e^{k+1},d_e^{k+1}+d_e^k\rangle-\frac{\tau}{2}\|Bu_e^{k+1}-d_e^{k+1}\|_2^2\\
&=\frac{\tau}{2}\|Bu_e^{k+1}\|_2^2+\frac{\tau}{2}\|Bu_e^{k+1}\|_2^2+\frac{\tau}{2}\|d_e^{k+1}\|_2^2+\frac{\tau}{2}\|d_e^{k+1}\|_2^2\\
&\quad-\tau\langle Bu_e^{k+1},d_e^{k+1}\rangle-\tau\langle Bu_e^{k+1},d_e^k\rangle-\frac{\tau}{2}\|Bu_e^{k+1}-d_e^{k+1}\|_2^2\\
&=\frac{\tau}{2}\|Bu_e^{k+1}\|_2^2+\frac{\tau}{2}\|d_e^{k+1}\|_2^2-\tau\langle Bu_e^{k+1},d_e^k\rangle+\frac{\tau}{2}\|d_e^k\|_2^2-\frac{\tau}{2}\|d_e^k\|_2^2\\
&=\frac{\tau}{2}\|Bu_e^{k+1}-d_e^k\|_2^2+\frac{\tau}{2}\|d_e^{k+1}\|_2^2-\frac{\tau}{2}\|d_e^k\|_2^2.
\end{aligned}\tag{4.11}$$

Substituting (4.10) and (4.11) into (4.9), we obtain

$$\begin{aligned}
0=&\lambda\|Du_e^{k+1}\|_2^2+\langle p^{k+1}-p^*,h_e^{k+1}\rangle+\mu\langle q^{k+1}-q^*,d_e^{k+1}\rangle\\
&+\frac{\gamma}{2}\Big(\|b_e^{k+1}\|_2^2-\|b_e^k\|_2^2\Big)+\frac{\gamma}{2}\|Au_e^{k+1}-h_e^k\|_2^2+\frac{\gamma}{2}\|h_e^{k+1}\|_2^2-\frac{\gamma}{2}\|h_e^k\|_2^2\\
&+\frac{\tau}{2}\Big(\|c_e^{k+1}\|_2^2-\|c_e^k\|_2^2\Big)+\frac{\tau}{2}\|Bu_e^{k+1}-d_e^k\|_2^2+\frac{\tau}{2}\|d_e^{k+1}\|_2^2-\frac{\tau}{2}\|d_e^k\|_2^2.
\end{aligned}\tag{4.12}$$

By summing the equation (4.12) from k=0 to $k=K$, we obtain

$$\begin{aligned}
&\frac{\gamma}{2}\Big(\|b_e^0\|_2^2+\|h_e^0\|_2^2\Big)+\frac{\tau}{2}\Big(\|c_e^0\|_2^2+\|d_e^0\|_2^2\Big)\\
&=\sum_{k=0}^{K}\lambda\|Du_e^{k+1}\|_2^2+\sum_{k=0}^{K}\langle p^{k+1}-p^*,h_e^{k+1}\rangle+\mu\sum_{k=0}^{K}\langle q^{k+1}-q^*,d_e^{k+1}\rangle\\
&\quad+\frac{\gamma}{2}\Big(\|b_e^{k+1}\|_2^2+\|h_e^{k+1}\|_2^2\Big)+\frac{\gamma}{2}\sum_{k=0}^{K}\|Au_e^{k+1}-h_e^k\|_2^2\\
&\quad+\frac{\tau}{2}\Big(\|c_e^{k+1}\|_2^2+\|d_e^{k+1}\|_2^2\Big)+\frac{\tau}{2}\sum_{k=0}^{K}\|Bu_e^{k+1}-d_e^k\|_2^2.
\end{aligned}\tag{4.13}$$

Since $p^{k+1}\in\partial\Big(\|h^{k+1}\|_1\Big)$, $p^*\in\partial\Big(\|h^*\|_1\Big)$ and $\|\cdot\|_1$ is convex, by Lemma 2.2 we have

$$\langle p^{k+1}-p^*,h_e^{k+1}\rangle\geq 0.$$

Since $q^{k+1}\in\partial\varphi(d^{k+1})$, $q^*\in\partial\varphi(d^*)$ and $\varphi(\cdot)$ is convex, by Lemma 2.2 we also have

$$\langle q^{k+1}-q^*,d_e^{k+1}\rangle\geq 0.$$

Hence all terms involved in (4.13) are non-negative.

From (4.13), we can obtain the following inequality

$$\frac{\gamma}{2}\Big(\|b_e^0\|_2^2+\|h_e^0\|_2^2\Big)+\frac{\tau}{2}\Big(\|c_e^0\|_2^2+\|d_e^0\|_2^2\Big)\geq\sum_{k=0}^{K}\lambda\|Du_e^{k+1}\|_2^2\quad\text{for every } K.\tag{4.14}$$

Taking the limit of $K\to\infty$ for the inequality (4.14) yields

$$\sum_{k=0}^{\infty}\lambda\|Du_e^{k+1}\|_2^2\leq\frac{\gamma}{2}\Big(\|b_e^0\|_2^2+\|h_e^0\|_2^2\Big)+\frac{\tau}{2}\Big(\|c_e^0\|_2^2+\|d_e^0\|_2^2\Big)<\infty.$$

From this inequality, one can easily obtain

$$\lim_{k\to\infty}\lambda\|Du_e^{k+1}\|_2^2=\lim_{k\to\infty}\lambda\langle D^TDu^{k+1}-D^TDu^*,u^{k+1}-u^*\rangle=0.\tag{4.15}$$

On the other hand, we have the following identity

$$\begin{aligned}
&B_{\frac{1}{2}\|D(\cdot)\|_2^2}^{D^TDu^*}(u^k,u^*)+B_{\frac{1}{2}\|D(\cdot)\|_2^2}^{D^TDu^k}(u^*,u^k)\\
&=\frac{1}{2}\|Du^k\|_2^2-\frac{1}{2}\|Du^*\|_2^2-\langle u^k-u^*,D^TDu^*\rangle+\frac{1}{2}\|Du^*\|_2^2-\frac{1}{2}\|Du^k\|_2^2-\langle u^*-u^k,D^TDu^k\rangle\\
&=\langle D^TDu^k-D^TDu^*,u^k-u^*\rangle.
\end{aligned}\tag{4.16}$$

Since the Bregman distances are non-negative, from (4.15) and (4.16)

$$\lim_{k\to\infty} \lambda B^{D^T Du^*}_{\frac{1}{2}\|D(\cdot)\|_2^2}(u^k, u^*) = 0. \tag{4.17}$$

That is, we obtain

$$\lim_{k\to\infty} \lambda\Big(\frac{1}{2}\|Du^k\|_2^2 - \frac{1}{2}\|Du^*\|_2^2 - \langle u^k - u^*, D^T Du^*\rangle\Big) = 0. \tag{4.18}$$

From (4.13), one can obtain the following inequality

$$\frac{\gamma}{2}\Big(\|b_e^0\|_2^2 + \|h_e^0\|_2^2\Big) + \frac{\tau}{2}\Big(\|c_e^0\|_2^2 + \|d_e^0\|_2^2\Big) \geq \sum_{k=0}^{K}\langle p^{k+1} - p^*, h_e^{k+1}\rangle \text{ for every } K. \tag{4.19}$$

Taking the limit of $K \to \infty$ for (4.19), we obtain

$$\sum_{k=0}^{\infty}\langle p^{k+1} - p^*, h_e^{k+1}\rangle \leq \frac{\gamma}{2}\Big(\|b_e^0\|_2^2 + \|h_e^0\|_2^2\Big) + \frac{\tau}{2}\Big(\|c_e^0\|_2^2 + \|d_e^0\|_2^2\Big) < \infty,$$

which implies

$$\lim_{k\to\infty}\langle p^k - p^*, h_e^k\rangle = 0. \tag{4.20}$$

On the other hand, we have the following identity

$$B^{p^*}_{\|\cdot\|_1}(h^k, h^*) + B^{p^k}_{\|\cdot\|_1}(h^*, h^k) = \langle p^k - p^*, h_e^k\rangle.$$

Using (4.20) and non-negativity of the Bregman distance, we obtain

$$\lim_{k\to\infty} B^{p^*}_{\|\cdot\|_1}(h^k, h^*) = \lim_{k\to\infty}(\|h^k\|_1 - \|h^*\|_1 - \langle h^k - h^*, p^*\rangle) = 0. \tag{4.21}$$

From (4.13), one obtains the following inequality

$$\frac{\gamma}{2}\Big(\|b_e^0\|_2^2 + \|h_e^0\|_2^2\Big) + \frac{\tau}{2}\Big(\|c_e^0\|_2^2 + \|d_e^0\|_2^2\Big) \geq \mu\sum_{k=0}^{K}\langle q^{k+1} - q^*, d_e^{k+1}\rangle \text{ for every } K. \tag{4.22}$$

From (4.22), we can obtain

$$\mu \lim_{k\to\infty}\langle q^k - q^*, d_e^k\rangle = 0. \tag{4.23}$$

Since $B^{q^*}_{\varphi(\cdot)}(d^k, d^*) + B^{q^k}_{\varphi(\cdot)}(d^*, d^k) = \langle q^k - q^*, d_e^k\rangle$ and the Bregman distances are non-negative, from (4.23) one can obtain

$$\lim_{k\to\infty} \mu B^{q^*}_{\varphi(\cdot)}(d^k, d^*) = \mu \lim_{k\to\infty}\Big(\varphi(d^k) - \varphi(d^*) - \langle d^k - d^*, q^*\rangle\Big) = 0. \tag{4.24}$$

From (4.13), we can also obtain the following properties

$$\lim_{k\to\infty}\|Bu_e^{k+1} - d_e^k\|_2 = 0, \tag{4.25}$$

$$\lim_{k\to\infty}\|Au_e^{k+1} - h_e^k\|_2 = 0. \tag{4.26}$$

Since $Bu_e^{k+1} - d_e^k = Bu^{k+1} - d^k$ and $h^* = Au^* - f$, (4.25) and (4.26) imply

$$\lim_{k\to\infty}\|Bu^{k+1} - d^k\|_2 = 0, \tag{4.27}$$

$$\lim_{k\to\infty}\|(Au^{k+1} - f) - h^k\| = 0. \tag{4.28}$$

Since $\varphi(\cdot)$ is continuous and $d^* = Bu^*$, by (4.24) and (4.27) we obtain

$$\mu \lim_{k\to\infty}\Big(\varphi(Bu^k) - \varphi(Bu^*) - \langle Bu^k - Bu^*, q^*\rangle\Big) = 0. \tag{4.29}$$

Since $\|\cdot\|_1$ is continuous, by (4.21) and (4.28)

$$\begin{aligned}&\lim_{k\to\infty}\Big(\|Au^k-f\|_1-\|Au^*-f\|_1-\langle(Au^k-f)-(Au^*-f),\ p^*\rangle\Big)\\&=\lim_{k\to\infty}\Big(\|Au^k-f\|_1-\|Au^*-f\|_1-\langle u^k-u^*,A^Tp^*\rangle\Big)=0.\end{aligned}\tag{4.30}$$

Summing (4.18), (4.29) and (4.30), one obtains

$$\begin{aligned}&\lim_{k\to\infty}\lambda\Big(\frac{1}{2}\|Du^k\|_2^2-\frac{1}{2}\|Du^*\|_2^2-\langle u^k-u^*,D^TDu^*\rangle\Big)\\&+\lim_{k\to\infty}\mu\Big(\varphi(Bu^k)-\varphi(Bu^*)-\langle Bu^k-Bu^*,\ q^*\rangle\Big)\\&+\lim_{k\to\infty}\Big(\|Au^k-f\|_1-\|Au^*-f\|_1-\langle u^k-u^*,A^Tp^*\rangle\Big)=0.\end{aligned}\tag{4.31}$$

Rearranging (4.31), one obtains

$$\begin{aligned}\lim_{k\to\infty}\Big(&\|Au^k-f\|_1+\frac{\lambda}{2}\|Du^k\|_2^2+\mu\varphi(Bu^k)\\&-\|Au^*-f\|_1-\frac{\lambda}{2}\|Du^*\|_2^2-\mu\varphi(Bu^*)\\&-\langle u^k-u^*,\lambda D^TDu^*+A^Tp^*+\mu B^Tq^*\rangle\Big)=0.\end{aligned}\tag{4.32}$$

Since $\lambda D^TDu^*+A^Tp^*+\mu B^Tq^*=0$ from (4.2), (4.32) gives

$$\lim_{k\to\infty}\|Au^k-f\|_1+\frac{\lambda}{2}\|Du^k\|_2^2+\mu\varphi(Bu^k)=\|Au^*-f\|_1+\frac{\lambda}{2}\|Du^*\|_2^2+\mu\varphi(Bu^*),\tag{4.33}$$

which completes the proof.

REFERENCES

[1] A. Bjorck, *Numerical methods for least squares problems,* SIAM, Philadelphia **1996**.

[2] J.F. Cai, S. Osher and Z. Shen, *Split Bregman methods and frame based image restoration,* Multiscale Model. Simul. **2009** (8), 337-369.

[3] A. Chambolle and T. Pock *A first-order primal-dual algorithm for convex problems with applications to imaging,* J. Math. Imageing Vis. **2011** (40), 120-145.

[4] C.L.P. Chen, L. Liu, L. Chen, and Y.Y. Tang *Weighted couple sparse representation with classified regularization for impulse noise removal,* IEEE Trans. Image Process. **2015** (24), 4014-4026.

[5] Y. Dong, M. Hintermuüller and M. Neri *An efficient primal-dual hybrid gradient algorithm for total variation image restoration,* SIAM J. Appl. Math. **2005** (65), 1817-1837.

[6] T. Goldstein and S. Osher *The split Bregman method for L1-regularized problems,* SIAM J. Imaging Sci. **2009** (2), 323-343.

[7] Y.D. Han and J.H. Yun, *Performance of fixed-point-like methods for a TVL1 problem with impulse noise*, Int. J. Eng. Res. Tech. **2019** (12), 2431-2438.

[8] J. Lu, K. Qiao, L. Shen and Y. Zou, *Fixed point algorithm for a TVL1 image restoration model,* Int. J. Comput. Math. **2018** (95), 1829-1844.

[9] C.A. Micchelli, L. Shen, Y. Xu and X. Zeng *Proximity algorithms for the L1/TV image denoising model,* Adv. Comput. Math. **2013** (38), 401-426.

[10] M. Nikolova *A variational approach to remove outliers and impulse noise,* J. Math. Iamgeing Vis. **2004** (20), 99-120.

[11] X. Li *Fine-granularity and spatially-adaptive regularization for projection-based image deblurring,* IEEE Trans. Image Process. **2011** (20), 971-983.

[12] J. Yang, Y. Zhang and W. Yin *An efficient TVL1 algorithm for deblurring multichannel images corrupted by impulsive noise,* SIAM. J. Sci. Computing **2009** (31), 2842-2865.

[13] J.H. Yun, *Image denoising methods for new TVL1 models with impulse noise*, Int. J. Eng. Res. Tech. **2020** (13), 686-698.

[14] J.H Yun and H.J. Lim *Image Restoration Using Fixed-Point-Like Methods for New TVL1 Variational Problems,* Electrionics **2020** (9), Article No. 735 (17 pages).